

A Study on Conjugate Heat Transfer Analysis of Reactor Vessel including Irradiated Structural Heat Source

Kunwoo Yi*, Hyuksu Cho, Inyoung Im, Eunkee Kim

KEPCO Engineering and Construction Company, 989-113 daedukdaero, Yuseong-gu, Daejeon, Korea

*Corresponding author: kwyi@kepc-enc.com

1. Introduction

Recently, Electric Power Research Institute, Inc. (EPRI) started the researches on aging management for pressurized water reactor internals and published several material reliability programs (MRPs) to provide the guidelines for the evaluation and methodologies and procedures of aging management for operating RVI [1,2]. Even though the MRPs have a purpose to provide the evaluation or management methodologies for the operating RVI, the similar evaluation methodologies can be applied to the APR1400 fleet in the design stage for the evaluation of neutron irradiation effects.

The purposes of this study are: to predict the thermal behavior whether or not irradiated structure heat source; to evaluate effective thermal conductivity (ETC) in relation to isotropic and anisotropic conductivity of porous media for APR1400 Reactor Vessel.

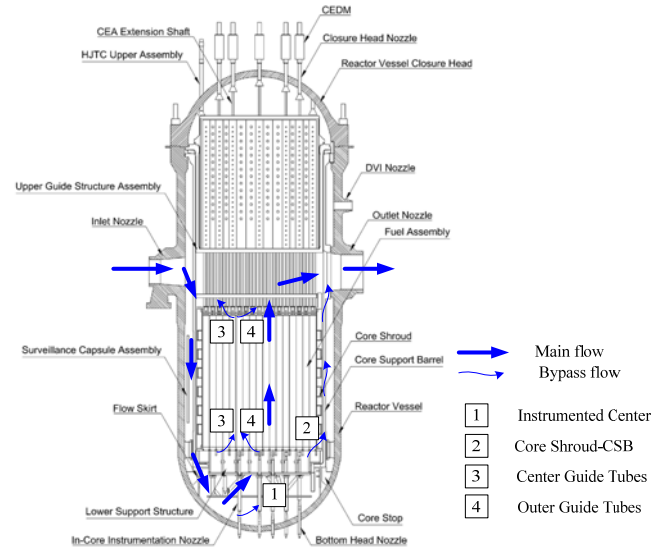


Fig. 1 Flow paths in the Reactor Vessel

2. Methods and Results

2.1 Configuration of Geometric Model

The APR1400 reactor vessel internals (RVI) consist of two major structures, the core support structures and internal structures. The RVIs are composed of core support barrel (CSB) assembly, the lower support structure (LSS) and in-core instrumentation (ICI) nozzle assembly, and the core shroud (CS). The general arrangement of the APR1400 reactor is shown in Fig. 1 and Fig. 2.

2.2 Simulation Parameters

The numerical analysis is performed for the normal operation condition. A reactor coolant temperature goes up while passing through the reactor core, which release heat of 996 MWth that is the amount of heat generation from one quarter core model. Also a thermal porous media methodology is applied to experimental data for the reactor fuel. A working fluid is water and flow rate, thermal power and operating pressure are shown in Table I.

The reactor outside is thermally shielded and there is no heat escape. The inlet flow corresponds to the flow rate of one reactor coolant pump, 5,231.2 kg/s.

The irradiated heat amount obtained by MCNP neutron analysis[5] is mapped into solid grid structure using interpolation scheme.

Table I. Parameters of the reactor analysis

	Value	Unit
Thermal power	996	MWth
Operation pressure	15.51	MPa
Temperature (T_{cold})	290.6	°C
Mass flow rate	5,231.2	kg/s

2.3 Effective Thermal Conductivity for Fuel Model

The effective thermal conductivity of the fuel core is defined as a volume ratio of fluid and structure. This value is mainly used to mix the thermal conductivity of the solid and fluid materials [3].

The thermal conductivity of such material is direction dependent.

$$\rho_s c_{ps} (1-\varepsilon) \frac{\partial \langle T \rangle^s}{\partial t} = k_s (1-\varepsilon) \nabla^2 \langle T \rangle^s - \nabla \cdot \left[\frac{1}{V} \int_s k_s T ds \right] - \frac{1}{V} \int_s k_s T ds \quad (1)$$

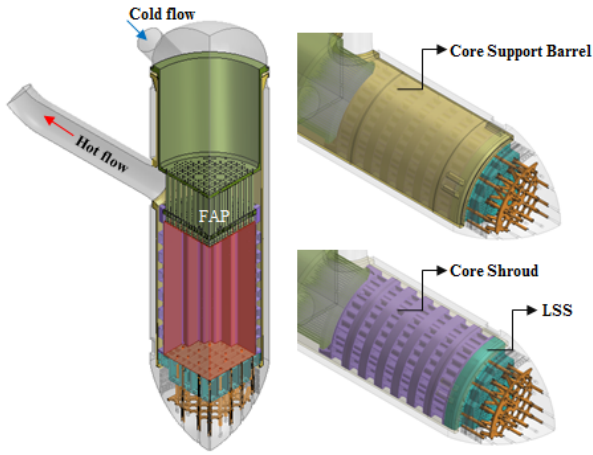


Fig. 2 Geometry model of the RVI

$$(\rho c_p)_{sf} = (1-\varepsilon)\rho_s c_{ps} + \varepsilon\rho_f c_{pf} \quad (2)$$

Case A (isotropic tensor):

$$k_{sf,xx-yy-zz} = (1-\varepsilon)k_s + \varepsilon k_f \quad (3)$$

Case B (anisotropic tensor):

$$k_{sf,yy} = (1-\varepsilon)k_s + \varepsilon k_f \quad (4)$$

$$k_{sf,xx-yy} = k_f \left(1 + \frac{2\varepsilon}{C_1 - \varepsilon + C_2(0.30584\varepsilon^4 + 0.013363\varepsilon^8 + \dots)} \right) \quad (5)$$

$$C_1 = \frac{k_s + k_f}{k_s - k_f} \quad C_2 = \frac{k_s - k_f}{k_s + k_f}$$

ε : Porosity

k_s, k_f : Thermal conductivity of solid and fluid

$xx - yy - zz$: coordinate direction

2.4 Result

CFD simulations were performed using the commercial code, STAR-CCM+ [4]. For the best computational accuracy, a polyhedral mesh was chosen so as to predict wall bounded turbulent flow.

When compared to a tetrahedral or hexahedral cell, a polyhedral cell has more faces, and therefore it has more optimal flow directions (normal to a face) than a tetrahedral or hexahedral cell. The polyhedral cells have more neighbors which allows for better gradient approximations, especially near boundaries and corners.

As a starting point, a mesh with $\sim 15 \times 10^6$ cells was generated with polyhedral cells, to be called the ‘‘Coarse’’ mesh case. After preliminary simulations and subsequent examinations of the y^+ values, two additional meshes were created. The ‘‘medium’’ mesh with $\sim 21 \times 10^6$ cells had further refinements in RVI internal structures in order to attain a maximum $y^+ > 30$. In the ‘‘fine’’ mesh case, additional

refinements were made to the cells in internal fluid volume and the prism-layer meshes on the fluid surface. This increased the total cell count to $\sim 37 \times 10^6$.

In order to evaluate mesh independence, all simulations were monitored with a maximum temperature and average absolute pressure in various regions of the flow path and internal solid structure. Three results of temperature and pressure are shown in Fig. 3 and 4 for $k-\omega$ and Realizable $k-\varepsilon$.

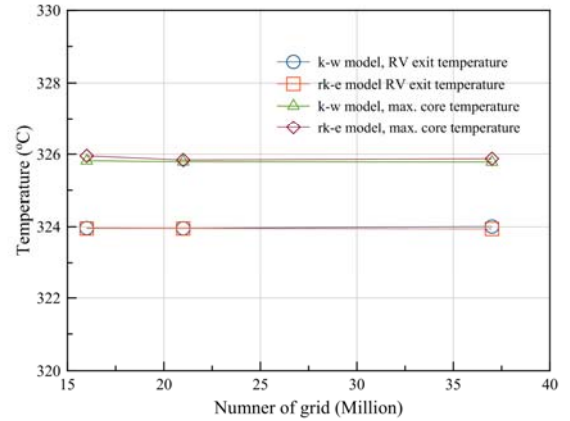


Fig. 3 Results of temperature for grid/turbulence test

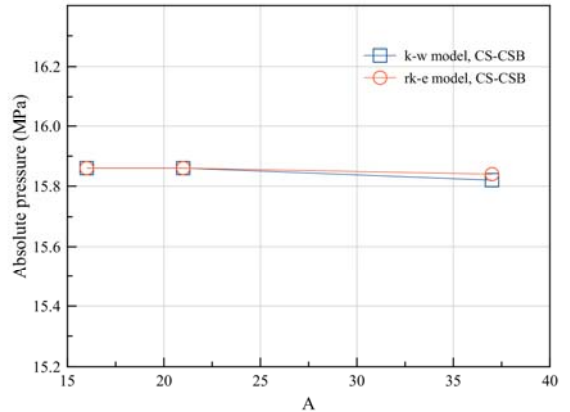


Fig. 4 Results of pressure for grid/turbulence test

As can be seen, there is no significant difference three mesh cases for temperature and pressure (RV exit temperature, fuel core temperature, 324 °C, 326 °C and CS-CSB average pressure, 15.8MPa), suggesting that the $k-\omega$ turbulence model and medium mesh case used in this study.

Table II and III are result for isotropic and anisotropic ETC regardless of irradiated structure heat source. In case of isotropic and anisotropic ETC, the maximum temperature of fluid and the core shroud without irradiated structure heat source are same, 325.7 °C. And the core shroud temperature has different, 0.5 °C. In respective of using irradiated heat source, the maximum temperature of fluid and the core shroud for isotropic ETC are 325.8 °C, 341.5 °C.

The maximum fluid and the core shroud temperature for anisotropic ETC are 325.7 °C, 341.4 °C. The

anisotropic ETC model does not well heat transfer to radial direction as a result.

The total amount of irradiated heat source is about 5.41 MWth and not effect to fluid temperature. The interior temperature of the core shroud is shown in Fig. 5 and Fig. 6.

3. Conclusions

The CFD simulations are performed so as to evaluate thermal behavior whether or not irradiated structure heat source and effective thermal conductivity for APR1400 Reactor Vessel.

In respective of using irradiated structure heat source, the maximum temperature of fluid and core shroud for isotropic ETC are 325.8 °C, 341.5 °C. The maximum temperature of fluid and core shroud for anisotropic ETC are 325.7 °C, 341.4 °C. The anisotropic ETC model does not well heat transfer across radial direction.

The total amount of irradiated structure heat source is about 5.41 MWth and not effect to fluid temperature.

REFERENCES

- [1] Materials Reliability Program: PWR Internals Material Aging Degradation Mechanism Screening and Threshold Values (MRP-175), EPRI, Palo Alto, CA: 2005. 1012081.
- [2] Materials Reliability Program: Functionality Analysis for Westinghouse and Combustion Engineering Representative PWR Internals (MRP-230, Revision 2), EPRI, Palo Alto, CA: 2012. 1021026
- [3] A review of model for effective thermal conductivity of composite materials, Journal of power Technologies 95, 2015
- [4] "STAR-CCM+, Version 8.02 USER GUIDE
- [5] "MCNP – A General Monte Carlo N-Particle Transport Code Version 5", Los Alamos National Laboratory Vols. I-III (April 2003)

Table II. Results of Case A (Isotropic)

	Fuel	Fluid	CS	CSB	LSS	UGS
w/o solid heat source	325.8	325.7	319.1	323.1	291.7	327.1
solid heat source	325.9	325.8	341.5	341.8	295.7	329.1

Table III. Results of Case B (Anisotropic)

	Fuel	Fluid	CS	CSB	LSS	UGS
w/o solid heat source	325.8	325.7	318.6	323.5	291.7	326.8
solid heat source	325.8	325.7	341.4	341.8	295.7	329.3

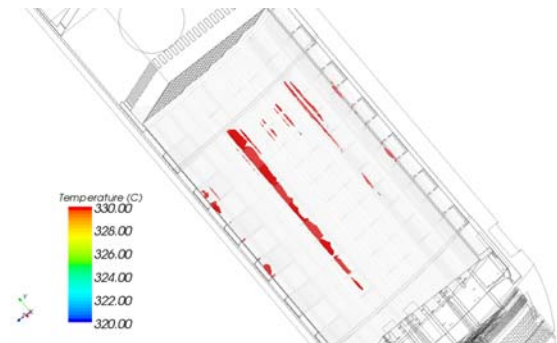


Fig. 5 Isotropic ETC for CS using irradiated heat source

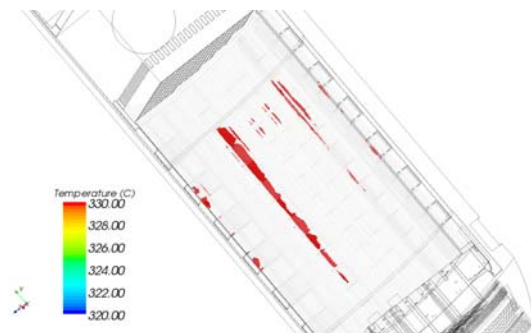


Fig. 6 Anisotropic ETC for CS using irradiated heat source